Porous Materials

DOI: 10.1002/ange.201107041

Three-Dimensional Ordered Arrays of 58 × 58 × 58 Å^3 Hollow Frameworks in Ionic Crystals of M_2Zn_2-Substituted Polyoxometalates**

*Kosuke Suzuki, Yuji Kikukawa, Sayaka Uchida, Hiroko Tokoro, Kenta Imoto, Shin-ichi Ohkoshi, and Noritaka Mizuno**

The design and synthesis of porous crystalline materials are of increasing interest because of the unique properties these materials have in sorption, separation, and catalysis.[1–3] Recent research has increased the diversity of porous crystalline materials by the rational control of the processes assembling the building blocks into inorganic zeolites and their analogues,[1] metal–organic frameworks (MOFs),[2] and covalent organic frameworks (COFs).[3] Polyoxometalates (POMs), anionic early transition-metal oxide clusters, are attractive building blocks for the construction of porous ionic crystals because of their rigid structures and redox, photochemical, and catalytic properties.[4] Multidentate anionic POMs with appropriate cations, self-assemble into porous crystalline materials, which show characteristic properties associated with the configuration of their pores, the types of POMs, and the type of metal atom in the POMs.[5] The pore and void sizes of the POM-based ionic crystals are less than 15 Å owing to strong and isotropic coulombic interactions. Although inorganic–organic ionic crystals based on POMs offer significant potential for the formation of novel porous materials, the introduction of large pores into ionic crystals is still a challenging task. Heterometallic POMs have not been used for the formation of porous ionic crystals, despite the potential they offer to control the physical properties by varying the metal atoms. This lack of use is because of the difficulty in precisely controlling the arrangements of different transition-metal atoms in POMs. The preparation of heterometallic POMs has only been carried out by multistep substitution methods:[6] one or two vacant sites of lacunary POMs are temporally blocked with removable alkali-metal ions (Na^+ or K^+) and the first inner transition-metal ions (M) are introduced. Then, the alkali-metal ions are replaced by the other transition metal ions (M′) to construct the $M_nM'_m$ cores.

Herein, we report a single-step synthesis of heterometallic M_2Zn_2-substituted POMs **1** ($M = Co^{II}$) and **2** ($M = Ni^{II}$), and an assembly of these heterometallic substituted POMs with tetrabutylammonium (TBA) cations into porous ionic crystals $TBA_8[\{M(OH_2)_2(\mu_3\text{-}OH)\}_2\{Zn(OH_2)\}_2\{\gamma\text{-}HSiW_{10}O_{36}\}_2]\cdot n\,EtOAc\cdot m\,H_2O$ (TBA-**1**; M = Co and TBA-**2**; M = Ni; Figure 1). TBA-**1** and TBA-**2** possess 58 × 58 × 58 Å^3 cage-like frameworks with approximately 38 × 38 × 38 Å^3 large spherical voids, where about 60 EtOAc and 144 H_2O solvent molecules reside. The voids are connected by three-dimensional channels, and guest molecules have easy access to the voids to conduct the guest-exchange while maintaining the porous crystalline structures. The tetranuclear Zn core of Zn_4-substituted POM (**3**) $[\{Zn(OH_2)(\mu_3\text{-}OH)\}_2\{Zn(OH_2)_2\}_2\{\gamma\text{-}HSiW_{10}O_{36}\}_2]^{8-}$ has two types of Zn atoms: the two central Zn atoms are octahedrally six-coordinate and side two Zn atoms are tetrahedrally coordinated to four oxygen atoms

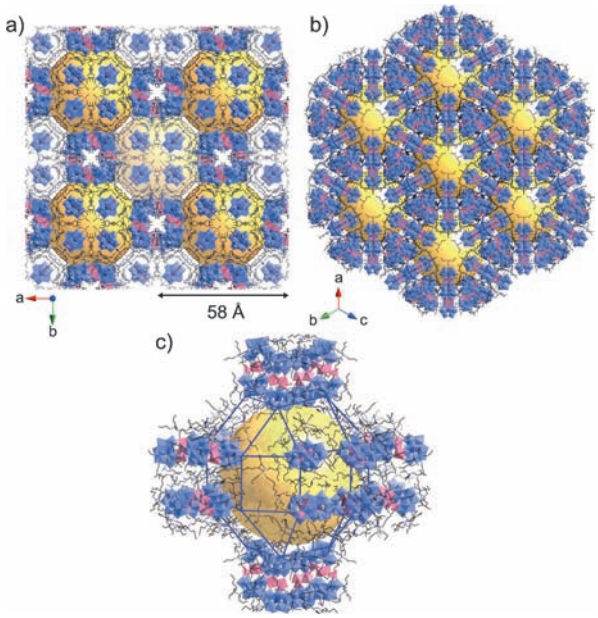

Figure 1. Crystal structure of TBA-**1**–**3** along the a) *a* axis, b) [111] direction, and c) representation around a rhombicuboctahedron. Yellow spheres represent inner voids (ca. 38 × 38 × 38 Å^3).

[*] Dr. K. Suzuki, Dr. Y. Kikukawa, Dr. S. Uchida, Prof. Dr. N. Mizuno
Department of Applied Chemistry, School of Engineering, The University of Tokyo
7-3-1 Hongo, Bunkyo-ku, Tokyo 113-8656 (Japan)
E-mail: tmizuno@mail.ecc.u-tokyo.ac.jp
Dr. H. Tokoro, K. Imoto, Prof. Dr. S. Ohkoshi
Department of Chemistry, School of Science, The University of Tokyo
7-3-1 Hongo, Bunkyo-ku, Tokyo 113-0033 (Japan)

[**] This work was supported by the Global COE Program (Chemistry Innovation through Cooperation of Science and Engineering), Grant-in-Aid for Scientific Research from the Ministry of Education, Culture, Science, Sports, and Technology of Japan (MEXT), Funding Program for World-Leading Innovative R&D on Science and Technology (FIRST Program). M = Co, Ni, Zn.

Supporting information for this article is available on the WWW under http://dx.doi.org/10.1002/anie.201107041.

(Figure 2).[7] The two different coordination sites of the tetranuclear core provide the idea for a single-step synthetic strategy for heterometallic transition-metal cores (M_2Zn_2) by

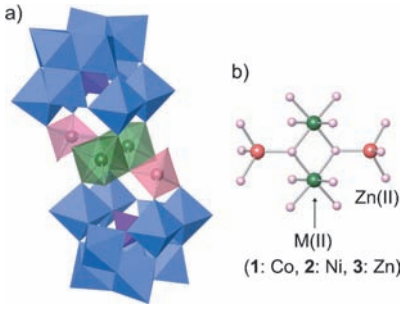

Figure 2. a) Enlarged POM unit of **1**–**3**, metal substituents shown as green and pink polyhedra, rest of the POM in blue/purple. and b) the central tetranuclear $\{M(OH_2)_2(\mu_3\text{-}OH)\}_2\{Zn(OH_2)\}_2$ core of POM (M = Co (**1**), Ni (**2**), Zn (**3**)).

simply mixing equimolar amounts of $[\gamma\text{-}SiW_{10}O_{36}]^{8-}$, tetrahedral Zn, and octahedral metal species (Co^{II} or Ni^{II}). Thus a 1/1 mixture of $Co(acac)_2/Zn(acac)_2$ (for **1**; acac = acetylacetone) or $Ni(acac)_2/Zn(acac)_2$ (for **2**) was added to a TBA salt of a dilacunary $[\gamma\text{-}SiW_{10}O_{36}]^{8-}$ in acetone. After 10 min, the positive-ion cold-spray ionization mass (CSI-MS) spectrum of **1** showed prominent signals for $[(TBA)_9H_2Co_2Zn_2(SiW_{10}O_{36})_2(OH)_2]^+$ *m/z* 7351.7 (calcd 7351.9) and $[(TBA)_{10}H_2Co_2Zn_2(SiW_{10}O_{36})_2(OH)_2]^{2+}$ *m/z* 3796.4 (calcd 3796.9) and no peaks other than the Co_2Zn_2 core were observed (Supporting Information, Figure S1), indicating quantitative formation of a dimeric structure of a silicotungstate with a heterometallic tetranuclear Co_2Zn_2 core. The isotopic distribution of the signals agreed well with the simulated patterns, indicating that these signals were not derived from a mixture of the related structural analogues (e.g., Co_4, Co_3Zn, $CoZn_3$, and Zn_4). The CSI-MS spectrum of **2** showed a signal for $[(TBA)_9H_2Ni_2Zn_2(SiW_{10}O_{36})_2(OH)_2]^+$ *m/z* 7350.6 (calcd 7350.9, Supporting Information, Figure S2), also indicating quantitative formation of **2**.

The anion structures of POMs **1** and **2** were successfully determined by single-crystal X-ray diffraction, UV/Vis spectra, elemental analyses, and magnetic susceptibility analyses. The rhombic dodecahedral single crystals suitable for diffraction were obtained by addition of ethyl acetate (EtOAc) into the synthetic solution. Crystal structures of **1** and **2** showed that the respective tetranuclear metal cores Co_2Zn_2 and Ni_2Zn_2 were sandwiched between two $[\gamma\text{-}SiW_{10}O_{36}]^{8-}$ units and that the two internal metal atoms were octahedrally six-coordinate, while the two side metal atoms were tetrahedrally four-coordinate to oxygen atoms. The molecular shapes of the anions were almost identical to that of Zn_4-substituted POM **3**. Elemental analyses showed the Si:W:Zn:M (M = Co, Ni) ratios of 2:20:2:2 in good agreement with the 2:2 heterometallic core composition.

The UV/Vis spectrum of **1** in acetonitrile showed bands around 480 nm ($^4T_{1g}(F)\rightarrow{}^4T_{1g}(P)$, $\varepsilon = 40$) and 520 nm ($^4T_{1g}(F)\rightarrow{}^4A_{2g}(F)$, $\varepsilon = 44$) assignable to the transition of octahedral Co^{II} center (Supporting Information, Figure S3). On the other hand, the band of $^4A_2(F)\rightarrow{}^4T_1(P)$ transition of tetrahedral Co^{II} ($\varepsilon \approx 500$) around 660 nm was not observed. Similarly, the UV/Vis spectrum of **2** showed bands assignable to the transition of octahedral Ni^{II}. The absence of relatively strong bands characteristic of tetrahedral metal centers show that Co^{II} (**1**) and Ni^{II} (**2**) are octahedrally coordinated to oxygen atoms.

The magnetic susceptibility data of **1** and **2** (Figure 3) demonstrate ferromagnetic interactions between high-spin Co^{II}–Co^{II} ($J = 5.37\ cm^{-1}$) and Ni^{II}–Ni^{II} ($J = 10.8\ cm^{-1}$), respectively.[8,9] The interaction results from the 90–100° bridging angles of Co-O-Co (95.2, 96.2°) and Ni-O-Ni (94.1, 95.0°) at the center of tetranuclear cores.[10] The bond valence sum (BVS) values of the Co (2.04) and Zn (1.91–2.12) atoms in **1** and the Ni (1.97) and Zn (2.02–2.18) atoms in **2** indicate that the valence assignments are Co^{II}, Ni^{II}, and Zn^{II} in accord with the results of the UV/Vis and magnetic susceptibility analyses. The BVS values of the oxygen atoms in the Co-O-Co and Ni-O-Ni linkage are 1.20–1.22 and 1.15–1.21, respectively, showing that these oxygen atoms are μ_3-OH ligands. Therefore, the formulas can be expressed by $[\{M(OH_2)_2(\mu_3\text{-}OH)\}_2\{Zn(OH_2)_2\}_2\{\gamma\text{-}HSiW_{10}O_{36}\}_2]^{8-}$ (M = Co (**1**), Ni (**2**)). To our knowledge, this is the first report of the precise 3d–3d′ heterometallic substitution of POMs in an organic solvent by the single-step synthesis.

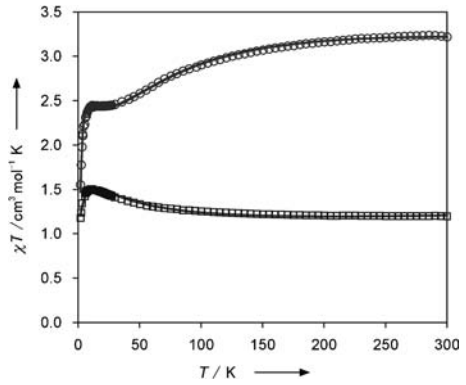

Figure 3. Temperature dependence of χT for polycrystalline samples of **1** (○, top) and **2** (□, bottom) in an applied field of 5000 Oe (The solid lines represent the best fits for the data).

The rigid POMs **1** or **2** with flexible TBA cations form porous ionic crystals with large hollow frameworks. Figure 1a and 1b show the packing structures of TBA-**1** (the corresponding structures for TBA-**2** and TBA-**3** are the same). The principle packing frameworks were "rhombicuboctahedral" when the inward-directed terminals of POMs were placed on the vertices of the framework (Figure 1c). In a unit cell, 24 POMs and 192 TBA surround the two voids (one at center and 8 × 1/8 at the corners of the unit cell). The dimension of the framework was $58 \times 58 \times 58\ Å^3$, and the diameter of the inner void was ca. $38 \times 38 \times 38\ Å^3$ (distance between diagonal POMs) as shown by yellow spheres in Figure 1. The closest distance between POMs was 7.3 Å and TBA cations lie between POMs. The large voids were three-dimensionally connected by channels with a diameter of approximately 8 Å.

The same porous packing structure was obtained from Zn_4-substituted POM TBA-**3** under the same solvent conditions (acetone/EtOAc).[11] To our knowledge, these are the largest pore and void sizes of the POM-based ionic crystals.

The solvent accessible volume of TBA-**3** estimated by PLATON[12] was 46% (90237 Å^3) of the total crystal volume (194623 Å^3). This void was occupied by disordered 60 EtOAc and 144 H_2O molecules (5 EtOAc and 12 H_2O per anion) as evidenced by thermogravimetric-differential thermal analysis (TG-DTA), elemental analysis, and ^{1}H NMR spectra of TBA-**3** dissolved in [D_6]DMSO. To avoid effects of paramagnetic metals, ^{1}H NMR and ^{13}C cross-polarization magic-angle spinning (CPMAS) NMR analyses were performed with diamagnetic TBA-**3**.

The mobility of EtOAc in the void was estimated by ^{13}C CPMAS NMR experiments, which provide information about the molecular dynamics in solid states by exploiting the fact that magnetic transfer from ^{1}H to ^{13}C is based on heteronuclear dipolar interactions. A signal intensity $I(t)$ in a ^{13}C CPMAS NMR spectrum is expressed by Equation (1) with an assumption $T_{CH} \ll T_{1\rho(H)}$, where I_o, T_{CH}, and $T_{1\rho(H)}$ represent the theoretical maximum signal intensity, cross-polarization time constants, and proton spin-lattice relaxation time, respectively.[13] The signal intensity of the less-mobile carbon atom reaches a maximum with a relatively short contact time (shorter T_{CH}). The changes in the ^{13}C CPMAS spectra of TBA-**3** with increasing contact times are shown in Supporting Information Figure S4. Only the signals of TBA cations were observed at short contact times (ca. 0.2 ms). At longer contact times (over 10 ms), the signals of TBA disappeared and those of EtOAc appeared (Figure 4). The cross-polarization time constants for the C1 and C2 carbon atoms in TBA were 0.20 and 0.25 ms, respectively, and these values are comparable to those of alkylammonium surfactants in mesoporous silica.[14] In contrasts, signals of EtOAc molecules in TBA-**3** showed longer cross-polarization time constants ($T_{CH} = 18$ ms), suggesting that EtOAc molecules have a high mobility in the large voids of TBA-**3**.

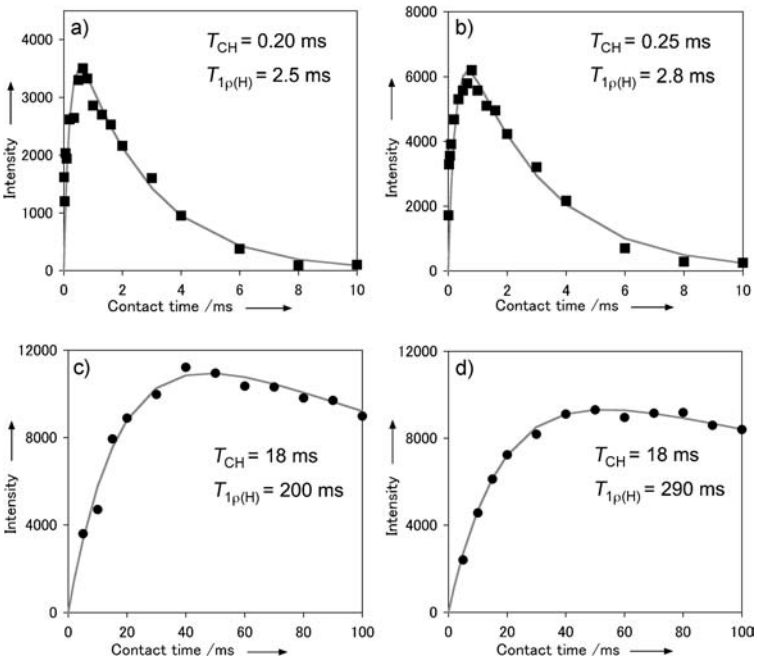

Figure 4. Signal intensities of ^{13}C CPMAS NMR spectra of TBA-**3** at room temperature as a function of contact time. a) C1 ($\delta = 57.2$ ppm) and b) C2 ($\delta = 23.9$ ppm) of TBA, c) methylene group ($\delta = 60.3$ ppm), and d) methyl group of acetate moiety ($\delta = 20.6$ ppm) of EtOAc.

$$I(t) = [I_o - (T_{CH}/T_{1\rho(H)})]^{-1}[\exp(-t/T_{1\rho(H)}) - \exp(-t/T_{CH})] \quad (1)$$

The high mobility of EtOAc in the voids enabled facile exchange with the other guest molecules through the three-dimensional channels. After TBA-**3** was immersed in dimethyl carbonate (DMC) for 12 h, the sample was collected and dried. The collected sample contained 108 DMC molecules per void and no EtOAc molecules, showing the exchange of EtOAc with DMC.[15] The powder X-ray diffraction (XRD) pattern after guest exchange was almost identical to that of TBA-**3** (Supporting Information Figure S5). These results showed that DMC molecules can access the void through the channels of TBA-**3**, and that guest-exchange proceeded without changing the framework of the structure. In a similar manner, toluene, *n*-butyl acetate, 2-hexanol, 2-octanol, and ethyl benzoate could access into the voids (ca. 100 molecules, Supporting Information Table S1).

In conclusion, we have prepared 3d–3d′ heterometallic arrangements of the tetranuclear cores (Co_2Zn_2 and Ni_2Zn_2) sandwiched between the dilacunary POM units in a single-step, and the molecular structures were successfully determined. Porous ionic crystals with rhombicuboctahedral large voids (TBA-**1**–**3**) are formed by the self-assembly of these tetranuclear metal substituted POMs with TBA cations. The guest molecules are highly mobile in the voids of the ionic crystals and can be exchanged by other molecules entering through the three-dimensional channels.

Experimental Section

TBA-**1**: $Zn(acac)_2$ (76.8 mg, 0.291 mmol), $Co(acac)_2{\cdot}2H_2O$ (85.4 mg, 0.291 mmol), and water (0.5 mL) were added to $TBA_4[\gamma\text{-}SiW_{10}O_{34}(H_2O)_2]{\cdot}H_2O$[4h] (1.00 g, 0.291 mmol) in acetone (30 mL), and the solution was stirred for 4 h at room temperature. After EtOAc (ca. 28 mL) was added, the solution was kept for 2 days. The pink crystals of TBA-**1** were obtained and dried under vacuum (621 mg, 0.0844 mmol, 58% yield). Positive-ion MS (CSI, acetone): *m*/*z* 7351.7 $TBA_9[HSiW_{10}O_{36}CoZn(OH)]_2^+$ (calcd 7351.9); elemental analysis before evacuation, calcd (%) for $C_{138}H_{348}Si_2N_8O_{97}W_{20}Zn_2Co_2$ ($TBA_8[\{Co(OH_2)_2(\mu_3\text{-}OH)\}_2\{Zn(OH_2)\}_2\{HSiW_{10}O_{36}\}_2]{\cdot}2.5\,EtOAc{\cdot}12\,H_2O$): C 21.66, H 4.58, N 1.46, Si 0.73, Co 1.54, Zn 1.71, W 48.04; found C 21.23, H 4.70, N 1.65, Si 0.72, Co 1.48, Zn 1.66, W 47.10.

TBA-**2**: $Zn(acac)_2$ (38.4 mg, 0.146 mmol), $Ni(acac)_2{\cdot}2H_2O$ (42.7 mg, 0.146 mmol), and water (0.25 mL) were added to $TBA_4[\gamma\text{-}SiW_{10}O_{34}(H_2O)_2]{\cdot}H_2O$ (500 mg, 0.146 mmol) in acetone (30 mL) and the solution was stirred for 4 h at room temperature. After EtOAc (ca. 28 mL) was added, the solution was kept for 2 days. The pale

green crystals of TBA-**2** were obtained and dried under vacuum (350 mg, 0.0475 mmol, 65 % yield). Positive ion MS (CSI, acetone): *m/z* 7350.6 $TBA_9[\{HSiW_{10}O_{36}NiZn(OH)\}_2]^+$ (calcd 7350.9); elemental analysis before evacuation, calcd (%) for $C_{148}H_{368}Si_2N_8O_{102}W_{20}Zn_2Ni_2$ ($TBA_8[\{Ni(OH_2)_2(\mu_3\text{-}OH)\}_2\{Zn(OH_2)\}_2\{HSiW_{10}O_{36}\}_2]\cdot 5\,EtOAc\cdot 12\,H_2O$): C 22.57, H 4.71, N 1.42, Si 0.71, Ni 1.49, Zn 1.66, W 46.69; found C 22.30, H 4.37, N 1.63, Si 0.71, Ni 1.48, Zn 1.63, W 47.00.

TBA-**3**: Synthesis and characterization of the anion structure were conducted according to our previous report,[7] and in this case the solvent was modified to prepare the porous crystals. $Zn(acac)_2$ (76.8 mg, 0.291 mmol) and water (0.25 mL) were added to $TBA_4[\gamma\text{-}SiW_{10}O_{34}(H_2O)_2]\cdot H_2O$ (500 mg, 0.146 mmol) in acetone (30 mL) and the solution was stirred for 4 h at room temperature. After EtOAc (ca. 28 mL) was added, the solution was kept for 2 days. The colorless crystals of TBA-**3** were obtained (350 mg, 0.0444 mmol, 61 % yield). positive ion MS (CSI, acetone): *m/z* 7364.5 $TBA_9[\{HSiW_{10}O_{36}Zn_2(OH)\}_2]^+$ (calcd 7364.9); elemental analysis calcd (%) for $C_{148}H_{368}Si_2N_8O_{102}W_{20}Zn_4$ ($TBA_8[\{Zn(OH_2)_2(\mu_3\text{-}OH)\}_2\{Zn(OH_2)\}_2\{HSiW_{10}O_{36}\}_2]\cdot 5\,EtOAc\cdot 12\,H_2O$): C 22.54, H 4.68, N 1.42, Si 0.71, Zn 3.32, W 46.62; found C 22.31, H 4.77, N 1.58, Si 0.72, Zn 3.28, W 49.99.

Crystal data for TBA-**1**: $C_{128}H_{318}Co_2N_8O_{82}Si_2W_{20}Zn_2$, cubic, space group $I\text{-}43m$, $a=b=c=58.1057(2)$ Å, $V=196180.7(12)$ Å^3, $Z=24$, $M_r=6943.14$, $\rho_{calcd}=1.410$ g cm^{-3}, $\mu=7.299$ mm^{-1}, $T=153$ K, 47007 reflections measured, of which 24414 were unique ($R_{int}=0.026$). $R_1(I>2\sigma(I))=0.064$, wR_2 (all data) $=0.235$ for 17903 observed reflections ($I>2\sigma(I)$).

Crystal data for TBA-**2**: $C_{128}H_{318}N_8Ni_2O_{82}Si_2W_{20}Zn_2$, cubic, space group $I\text{-}43m$, $a=b=c=58.1349(2)$ Å, $V=196476.6(12)$ Å^3, $Z=24$, $M_r=6942.70$, $\rho_{calcd}=1.408$ g cm^{-3}, $\mu=7.302$ mm^{-1}, $T=153$ K, 47071 reflections measured, of which 24449 were unique ($R_{int}=0.023$). $R_1(I>2\sigma(I))=0.080$, wR_2 (all data) $=0.304$ for 16829 observed reflections ($I>2\sigma(I)$).

Crystal data for TBA-**3**: $C_{128}H_{318}N_8O_{82}Si_2W_{20}Zn_4$, cubic, space group $I\text{-}43m$, $a=b=c=57.95150(10)$ Å, $V=194623.0(6)$ Å^3, $Z=24$, $M_r=6956.02$, $\rho_{calcd}=1.424$ g cm^{-3}, $\mu=7.403$ mm^{-1}, $T=103$ K, 46713 reflections measured, of which 24268 were unique ($R_{int}=0.026$). $R_1(I>2\sigma(I))=0.071$, wR_2 (all data) $=0.251$ for 18981 observed reflections ($I>2\sigma(I)$).

CCDC-846973 (TBA-**1**), -846974 (TBA-**2**), and -846975 (TBA-**3**) contain the supplementary crystallographic data for this paper. These data can be obtained free of charge from The Cambridge Crystallographic Data Centre via href = "http://www.ccdc.cam.ac.uk/cgi-bin/catreq.cgi" > www.ccdc.cam.ac.uk/data_request/cif.

Received: October 5, 2011
Revised: December 5, 2011
Published online: January 10, 2012

Keywords: nanostructures · organic–inorganic hybrid composites · polyoxometalates · porous materials · self-assembly

[1] a) R. A. van Santen, G. J. Kramer, *Chem. Rev.* **1995**, *95*, 637–660; b) A. Corma, *Chem. Rev.* **1995**, *95*, 559–614; c) J. M. Thomas, *Angew. Chem.* **1999**, *111*, 3800–3843; *Angew. Chem. Int. Ed.* **1999**, *38*, 3588–3628; d) A. P. Wight, M. E. Davis, *Chem. Rev.* **2002**, *102*, 3589–3614.

[2] a) D. J. Tranchemontagne, Z. Ni, M. O'Keeffe, O. M. Yaghi, *Angew. Chem.* **2008**, *120*, 5214–5225; *Angew. Chem. Int. Ed.* **2008**, *47*, 5136–5147; b) S. Kitagawa, R. Kitaura, S.-i. Noro, *Angew. Chem.* **2004**, *116*, 2388–2430; *Angew. Chem. Int. Ed.* **2004**, *43*, 2334–2375; c) G. Férey, *Chem. Soc. Rev.* **2008**, *37*, 191–214; d) L. J. Murray, M. Dincă, J. R. Long, *Chem. Soc. Rev.* **2009**, *38*, 1294–1314; e) Y. Inokuma, M. Kawano, M. Fujita, *Nat. Chem.* **2011**, *3*, 349–358.

[3] a) H. M. El-Kaderi, J. R. Hunt, J. L. Mendoza-Cortés, A. P. Côté, R. E. Taylor, M. O'Keeffe, O. M. Yaghi, *Science* **2007**, *316*, 268–272; b) A. P. Côté, A. I. Benin, N. W. Ockwig, M. O'Keeffe, A. J. Matzger, O. M. Yaghi, *Science* **2005**, *310*, 1166–1170.

[4] a) C. L. Hill, C. M. Prosser-McCartha, *Coord. Chem. Rev.* **1995**, *143*, 407–455; b) T. Okuhara, N. Mizuno, M. Misono, *Adv. Catal.* **1996**, *41*, 113–252; c) R. Neumann, *Prog. Inorg. Chem.* **1998**, *47*, 317–370; d) U. Kortz, A. Müller, J. van Slageren, J. Schnack, N. S. Dalal, M. Dressel, *Coord. Chem. Rev.* **2009**, *253*, 2315–2327; e) D.-L. Long, R. Tsunashima, L. Cronin, *Angew. Chem.* **2010**, *122*, 1780–1803; *Angew. Chem. Int. Ed.* **2010**, *49*, 1736–1758; f) A. Müller, E. Krickemeyer, J. Meyer, H. Bögge, F. Peters, W. Plass, E. Diemann, S. Dillinger, F. Nonnenbruch, M. Randerath, C. Menke, *Angew. Chem.* **1995**, *107*, 2293–2295; *Angew. Chem. Int. Ed. Engl.* **1995**, *34*, 2122–2124; g) H. N. Miras, G. J. T. Cooper, D.-L. Long, H. Bögge, A. Müller, C. Streb, L. Cronin, *Science* **2010**, *327*, 72–74; h) K. Kamata, K. Yonehara, Y. Sumida, K. Yamaguchi, S. Hikichi, N. Mizuno, *Science* **2003**, *300*, 964–966.

[5] a) M. Hölscher, U. Englert, B. Zibrowius, W. F. Hölderich, *Angew. Chem.* **1994**, *106*, 2552–2554; *Angew. Chem. Int. Ed. Engl.* **1994**, *33*, 2491–2493; b) M. I. Khan, E. Yohannes, D. Powell, *Inorg. Chem.* **1999**, *38*, 212–213; c) J.-H. Son, H. Choi, Y.-U. Kwon, *J. Am. Chem. Soc.* **2000**, *122*, 7432–7433; d) J.-H. Son, Y.-U. Kwon, *Inorg. Chem.* **2004**, *43*, 1929–1932; e) J.-H. Son, Y.-U. Kwon, *Inorg. Chem.* **2003**, *42*, 4153–4159; f) Y. Ishii, Y. Takenaka, K. Konishi, *Angew. Chem.* **2004**, *116*, 2756–2759; *Angew. Chem. Int. Ed.* **2004**, *43*, 2702–2705; g) S. Uchida, M. Hashimoto, N. Mizuno, *Angew. Chem.* **2002**, *114*, 2938–2941; *Angew. Chem. Int. Ed.* **2002**, *41*, 2814–2817; h) S. Uchida, R. Kawamoto, T. Akatsuka, S. Hikichi, N. Mizuno, *Chem. Mater.* **2005**, *17*, 1367–1375; i) C. Jiang, A. Lesbani, R. Kawamoto, S. Uchida, N. Mizuno, *J. Am. Chem. Soc.* **2006**, *128*, 14240–14241.

[6] a) T. M. Anderson, K. I. Hardcastle, N. Okun, C. L. Hill, *Inorg. Chem.* **2001**, *40*, 6418–6425; b) T. M. Anderson, X. Zhang, K. I. Hardcastle, C. L. Hill, *Inorg. Chem.* **2002**, *41*, 2477–2488; c) I. M. Mbomekalle, B. Keita, L. Nadjo, W. A. Neiwert, L. Zhang, K. I. Hardcastle, C. L. Hill, T. M. Anderson, *Eur. J. Inorg. Chem.* **2003**, 3924–3928; d) L. Ruhlmann, C. Costa-Coquelard, J. Canny, R. Thouvenot, *Eur. J. Inorg. Chem.* **2007**, 1493–1500; e) D. Schaming, J. Canny, K. Boubekeur, R. Thouvenot, L. Ruhlmann, *Eur. J. Inorg. Chem.* **2009**, 5004–5009; f) C. M. Tourné, G. F. Tourné, F. Zonnevijlle, *J. Chem. Soc. Dalton Trans.* **1991**, 143–155; g) R. Neumann, A. M. Khenkin, *Inorg. Chem.* **1995**, *34*, 5753–5760; h) I. M. Mbomekalle, B. Keita, M. Nierlich, U. Kortz, P. Berthet, L. Nadjo, *Inorg. Chem.* **2003**, *42*, 5143–5152; i) R. Cao, K. P. O'Halloran, D. A. Hillesheim, S. Lense, K. I. Hardcastle, C. L. Hill, *CrystEngComm* **2011**, *13*, 738–740.

[7] Y. Kikukawa, K. Yamaguchi, N. Mizuno, *Angew. Chem.* **2010**, *122*, 6232–6236; *Angew. Chem. Int. Ed.* **2010**, *49*, 6096–6100.

[8] The magnetic data of **1** were analyzed by using the analytic expression for a magnetically anisotropic distorted octahedral Co^{II} dimer, and the following best fitting parameters were obtained: $J=5.37$ cm^{-1}, $g_z=2.72$, $g_x=4.90$, $\chi_{TIP}=190\times10^{-6}$ cm^{3}mol^{-1}, $D=181.6$ cm^{-1}: a) M. E. Lines, *J. Chem. Phys.* **1971**, *55*, 2977–2984; b) H. Sakiyama, *Inorg. Chim. Acta* **2006**, *359*, 2097–2100.

[9] The magnetic data of **2** were analyzed by using the analytic expression for an octahedral Ni^{II} dimer assuming the isotropic spin-coupling Hamiltonian and considering zero-field splitting D. The following best fitting parameters were obtained: $J=10.8$ cm^{-1}, $g=2.01$, $\chi_{TIP}=430\times10^{-6}$ cm^{3}mol^{-1}, $D=6.9$ cm^{-1}, where J is exchange interaction parameter, g_x and g_z are the anisotropic g-factors, χ_{TIP} is temperature independent paramag-

netism, and *D* is zero-filed splitting: A. P. Ginsberg, R. L. Martin, R. W. Brookes, R. C. Sherwood, *Inorg. Chem.* **1972**, *11*, 2884 – 2889.

[10] 90 – 100° angles of Co^{II}-O-Co^{II} and Ni^{II}-O-Ni^{II} favor the orthogonality of the magnetic orbital and result in the ferromagnetic coupling as expected from the Goodenough – Kanamori rule: J. B. Goodenough, *Magnetism and the Chemical Bond*, Interscience, New York, **1963**.

[11] However, note that nonporous densely packed structures were obtained when **1**–**3** were crystallized in other solvents such as 1,2-dichloroethane/diethyl ether,[7] acetone/diethyl ether, and acetone/toluene. Tetraethylammonium salts of **1**–**3** or TBA salt of other dimeric polyoxometalates also gave nonporous structures, which showed that the presence of the M_2Zn_2-substituted POMs (M = Co, Ni, Zn), TBA cations, and EtOAc is essential for the construction of the large hollow structures.

[12] A. L. Spek, PLATON: A Multipurpose Crystallographic Tool, Utrecht University, Utrecht, The Netherlands, **2001**.

[13] a) W. Kolodziejski, J. Klinowski, *Chem. Rev.* **2002**, *102*, 613 – 628; b) S. H. Liang, I. D. Gay, *Langmuir* **1985**, *1*, 593 – 599.

[14] L.-Q. Wang, J. Liu, G. J. Exarhos, B. C. Bunker, *Langmuir* **1996**, *12*, 2663 – 2669.

[15] The ^{1}H NMR spectra of the collected sample in [D_6]DMSO showed the DMC signal and no EtOAc signals were observed, indicating the exchange of EtOAc with DMC. The amount of DMC per void was estimated by comparison of the integrated signal intensity with that of TBA. It was confirmed by the elemental analyses that the amount of TBA cations was unchanged by the guest-exchange experiments (N contents: before exchange 1.58 wt %, after exchange 1.60 wt %).

